Neutron spectroscopy of water dynamics in NaX and NaA zeolites

William A. Kamitakahara
NIST Center for Neutron Research, National Institute of Standards and Technology, Gaithersburg, Maryland 20899-6102, USA

Noboru Wada
Department of Mechanical Engineering, Toyo University, Saitama 350-8585, Japan

(Received 7 August 2007; published 7 April 2008)

We have investigated the dynamics of water molecules in zeolites NaA and NaX by high-resolution quasielastic neutron scattering methods. Between 260 and 310 K, the local translational diffusive motion of water in the zeolites is one to two orders of magnitude slower than in bulk water. The Q dependence of the scattering shows effects of confinement and the presence of both relatively mobile and immobile molecules. The speed of the diffusive motion depends strongly on hydration level. Comparison with other hydrated siliceous materials indicates that the host charge per water molecule is a major factor in determining the time scale of diffusion.

DOI: 10.1103/PhysRevE.77.041503 PACS number(s): 61.05.F−, 61.25.−f, 82.75.−z

I. INTRODUCTION

The dynamics of water molecules near surfaces, ions, and molecules have important manifestations in industrial processes, in geochemistry, and in life processes. In the studies reported here, we examine several of the factors influencing water dynamics in zeolites, a class of microporous materials widely employed in chemical separations, catalysis, and many other applications. The motion of water molecules in the pores and channels of zeolites are subject not only to geometrical confinement, but also to the chemical environment of the host structure. The circumstances of the water molecules have much in common with conditions in many other systems of current interest, e.g., porous glasses, clay minerals, hydrated polymers, and macromolecules. In each case, the water molecules experience not only geometrical constraints, but also chemical interactions that strongly influence their dynamics. Among these systems, zeolites present a particularly favorable case for quasielastic neutron scattering (QENS) [1] experiments. The scattering from water molecules is easily distinguished from the highly crystalline, nonhydrogenous host, and the geometrical constraints are well defined. However, relatively good energy resolution, on the order of a few μeV, is needed to provide detailed information about translational diffusive motions. In the current paper, we report the results of QENS experiments on the dynamics of water in NaA and NaX zeolites. In comparison with other QENS studies on these and related systems, i.e., water in porous silicate glasses [2–10], layered silicates [11–17], and zeolites [18–26], our more extensive data at high resolution (1 μeV, or 0.008 cm^{-1} full width at half maximum) allow us to gain insights on how the translational diffusive motion is influenced by hydration level, geometrical confinement, zeolite composition, and temperature. Our results are in good qualitative agreement with molecular dynamics simulations [27–30].

A. The structure of zeolites

Zeolites are typically highly crystalline aluminosilicate materials with frameworks composed of SiO_4 and AlO_4 tetrahedra. While the silica-based component results in an electrically neutral framework, the substitution of Al^{3+} for Si^{4+} produces a deficit of one electron per Al atom. The net charge on the anionic framework is balanced by cations within the cages of the zeolite structure. We report the results of inelastic and quasielastic neutron scattering experiments on water in two common zeolites, NaA and NaX, in which the charge-compensating cations are Na^+. Their structures are the cubic Linde type A, or LTA, structure for NaA [31,32] and the cubic faujasite (FAU) structure [33,34] for NaX.

The basic building block of both LTA and FAU structures is the sodalite cage, a roughly spherical unit consisting of 24T (tetrahedral, i.e., Si or Al) atoms and bridging oxygen atoms. In LTA, the sodalite units, or β cages, are joined in a cubic array, connected by rectangular prisms of bridging oxygen atoms. In the resulting structure [31], relatively large α cages, approximately 11 Å in diameter, are framed by the sodalite units. The openings between α cages have a diameter of approximately 4 Å. Most of the Na^+ cations reside on the interfaces between α and β cages, at the centers of approximately hexagonal rings in the framework. Others lie near the centers of the octagonal rings between α cages. With less certainty, a few other cations may be located in the α cages, or elsewhere in the structure. In the FAU structure [33] of NaX, the sodalite units are connected by hexagonal prisms in a more open array, reminiscent of the diamond structure, forming α cages about 14 Å in diameter. Some of the Na^+ ions in FAU reside at the centers of the hexagonal prisms, or within the sodalite cages, and are thus more sequestered from the water in the α cages than is the case for LTA. Other cations are located at the centers of hexagonal rings, or on the peripheries of the α cages. The Si/Al ratio is 1.0 for NaA, and 1.25 for our sample of NaX. The chemical composition for NaA can be written $Na_{96}Si_{96}Al_{96}O_{384}$, comprising eight α cages and eight α cages within a cubic cell, while the NaX composition is similarly $Na_{85}Si_{107}Al_{85}O_{384}$, corresponding to four α cages and four β cages.

X-ray and neutron diffraction investigations of hydrated NaA and NaX zeolites [31,32,34] are not completely definitive in their ability to reveal details of water positions, due to several limitations. Among the latter is the difficulty of distinguishing between scattering contributions from water oxygen atoms and sodium atoms. Another problem is the highly disordered environment of the absorbed water. However, the studies do show that, even at high hydration levels, the water

 ©2008 The American Physical Society

distribution is far from random within the α cages, with sites near the cage boundaries preferred. Sites assigned to water oxygen positions in the diffraction studies generally have low occupancies, between 0.1 and 0.6, with 0.3 being a typical value. For hydrated NaA, Gramlich and Meier [31] proposed a structure with most of the water located at the vertices of a distorted dodecahedron, with 20 vertices and a diameter of 7.7 Å. Within the β cages, water is assigned to positions at the vertices of a distorted tetrahedron. Other water molecules are tentatively located close to Na ions near the centers of the octagonal rings between α cages. A more recent study by Ikeda *et al.* [32], combining neutron and x-ray diffraction, is in broad agreement with the earlier single-crystal x-ray investigation, but locates at least an additional Na site near the centers of the octagonal rings and one additional water site. At lower water content, when there are just a few water molecules in each α cage, x-ray diffraction studies [35] on *X*- and *Y*-type zeolites show that water prefers to assume positions bridging two Na cations.

B. Neutron scattering from bulk and confined water

The scattering function $S(Q,\omega)$ from our zeolite samples is dominated by the contribution from the hydrogen component, since the cross section of H (80 b/atom) is much larger than those of the other atoms. The scattering from H is mainly incoherent, and consequently related to hydrogen single-particle motion. Among earlier QENS studies of water dynamics, those of Teixeira *et al.* [36] on bulk water and supercooled bulk water are noteworthy. Their spectra were analyzed in terms of a model in which rotational and translational motions of a water molecule may be decoupled, so that

$$S(Q,\omega) = S_R(Q,\omega) \otimes S_T(Q,\omega), \tag{1}$$

where $\otimes$ signifies a convolution in ω. While in the general case such a decoupling is questionable, it is clear that at sufficiently low temperature and small Q, effectively one observes only the translational part $S_T(Q,\omega)$. In the decoupled picture, for $Q<1.0$ Å^{-1}, the rotational scattering function $S_R(Q,\omega)$ has a delta function component that comprises 85% or more of the integrated intensity [2], while the remainder has a width much larger than $S_T(Q,\omega)$. Therefore under high-resolution conditions at small Q, one observes only $S_T(Q,\omega)$, which modulates the delta-function part of $S_R(Q,\omega)$. At larger Q, between 1.0 and 1.75 Å^{-1}, the rotational scattering is even broader, and appears as just a flat background on our spectra. We discuss this point further in the following section. We expect that the scattering function we measure with the backscattering spectrometer is essentially $S_T(Q,\omega)$.

The form of $S_T(Q,\omega)$ is modified by the effects of confinement. If the translational diffusive motion is restricted to a volume characterized by a probability density $P(r)$, then $S_T(Q,\omega)$ will have a purely elastic component $A(Q)\delta(\omega)$, where the elastic incoherent structure factor (EISF), $A(Q)$, is the Fourier transform of $P(r)$. In the event that confinement is not complete, but interconnected regions exist where the diffusion between such regions is much slower than within each region, then we would anticipate a component of the form $A(Q)b(Q,\omega)$, where $b(Q,\omega)$ characterizes the intercavity diffusion. In our experiments, we have conditions of resolution and temperature such that the quasielastic broadening of $S_T(Q,\omega)$ is observable, but not that of $b(Q,\omega)$. The scattering law expected for continuous random diffusion within a hard-walled spherical cavity has been treated by Volino and Dianoux [37]. Although their model is not precisely applicable to our experiments, it is useful to consider their expressions for the EISF and $Q=0$ limit of the quasielastic scattering, as we discuss later.

II. EXPERIMENT

A. Sample treatment

The samples, obtained from the Tohso Chemical Co., were hydrated in humid air at 295 K, attaining a mass gain of 20% over the samples in the completely dehydrated state in the case of NaA, and 22% and 28% for two samples of NaX. These mass gains imply that for an amount of zeolite corresponding to one α cage plus one β cage, there are 19 molecules of absorbed water in our NaA sample, and 42 and 53 molecules for our NaX samples at the two hydration levels. In the hydrated condition, each sample mass was 1.2 g, and formed into the shape of a cylindrical annulus approximately 30 mm in height and 25 mm diameter, within an aluminum foil envelope. The annular samples were sealed in thin-walled aluminum containers for the neutron measurements.

B. Quasielastic neutron scattering experiment

The high-flux backscattering spectrometer [38] (HFBS) at the NIST Center for Neutron Research was used to obtain most of the QENS data in this investigation. The instrument has a unique combination of very high energy resolution (less than 1 μeV), and rather good signal intensity, so that spectra with adequate statistics and a dynamic range of ± 11 μeV could be obtained in about six hours. For each zeolite sample, a low-temperature (100 K) spectrum was taken to accurately measure the resolution function for each detector on the sample itself. The instrument operates with incident neutron energy of 2.08 meV. It has eight detectors spanning a Q range from 0.25 to 1.75 Å^{-1}. For each sample, before obtaining quasielastic spectra on the HFBS, fixed-window elastic scans were performed. In these scans, the Doppler drive that modulates the energy transfer is turned off, so that only scattering near $E=0$ is recorded, while the sample temperature is slowly increased or decreased in small steps.

III. QENS RESULTS AND ANALYSIS

Figure 1 compares fixed-window elastic scans for two hydrated zeolites and a hydrated synthetic layered silicate (Na-fluor-tetra-silicic mica). The latter sample was kindly provided by TOPY Industries, Ltd. The curves for hydrated NaA and NaX are very similar, and grossly similar in shape to that of the hydrated layered material [15], but are displaced upward in temperature with respect to the latter by about 40 K.

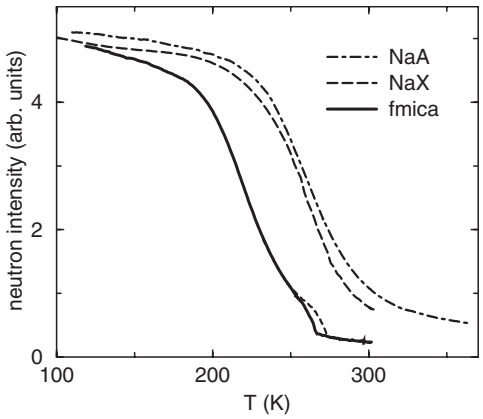

FIG. 1. Fixed-window elastic scans for three hydrated aluminosilicate systems. From top to bottom, the curves are for hydrated NaA and NaX zeolites, and a synthetic layered silicate (fluormica), heating (dashed line) and cooling (solid line). The hydration levels correspond to fractional mass gains of 0.20 for the NaA sample, 0.22 for the NaX sample, and 0.27 for the fluormica sample.

In each case, as quasielastic broadening increases with temperature, the neutron intensity within the 1 μeV resolution window drops until the scattering from the aqueous component is so broad that it no longer affects the intensity, and the only scattering remaining in the window is elastic scattering from the host material, plus background. The approach to the low intensity condition differs somewhat in the layered silicate compared to the zeolites. For the former, we observed additional structure around 270 K and hysteresis between heating and cooling. For the latter, no hysteresis was observed, and the approach to low intensity as temperature is increased is smooth and gradual. The comparative behavior is consistent with physical properties, since the fluormica readily desorbs all water at temperatures around 320 K in dry air, while NaA and NaX retain some water to much higher temperatures.

A typical QENS spectrum, shown in Fig. 2, can be fitted with just two components, a resolution-limited central part and a broader Lorentzian. Because the environment of water

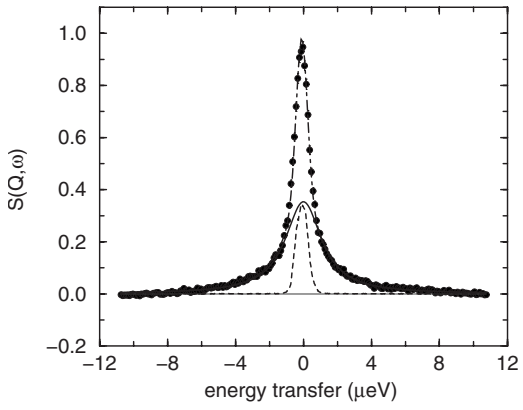

FIG. 2. Quasielastic scattering from water in NaA zeolite at 300 K, $Q=1.32$ Å^{-1}. The curves are, from top to bottom, the total fitted intensity, the Lorentzian component broadened by resolution, and the shape of the resolution function. Uncertainties due to counting statistics are approximately the size of the symbols.

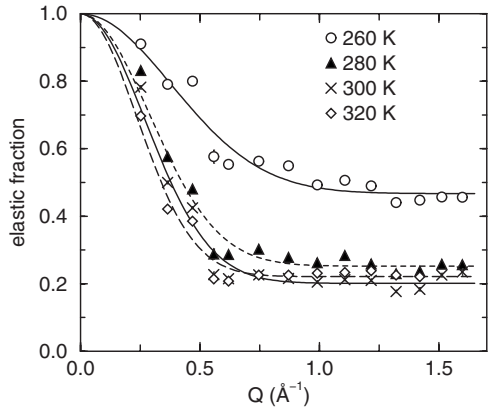

FIG. 3. Wave-vector dependence of the apparent elastic fraction for scattering from water in NaA zeolite. Fits are to a constant plus a Gaussian centered at $Q=0$. The hydration level corresponds to a fractional mass gain of 0.20 over the dry zeolite.

in zeolite systems is heterogeneous and complex, one expects in general more than one relaxation process and a more complicated QENS line shape than a single Lorentzian. However, the simple procedure that we have employed, which gives very good fits to the data in most cases, provides a convenient basis for comparing spectra at different wave vectors, temperatures, and hydration levels. Tests were carried out to determine to what extent the line shape we have chosen affects the interpretation of the data. In particular, we fit many of the spectra by assuming stretched-exponential relaxation, following other studies [8,10] of water in confinement. These fits are discussed later. As shown in Fig. 3, the apparent EISF (fraction of intensity that is in the resolution limited component) at each temperature displays an increase toward $Q=0$, and tends toward a constant at larger Q. The constant level indicates the presence of water that is immobile within the resolution of the instrument. The immobile water fraction is constant at temperatures of 280 K and above, but rises dramatically for 260 K. There is a strong rise of the apparent EISF at small Q, below 0.7 Å^{-1}, indicating that the local motion of the mobile water fraction is confined to a region of Å dimensions. Fitting a Gaussian line shape centered at $Q=0$ to the rise, and requiring that the EISF=1 at $Q=0$, we obtained the fits shown in Fig. 3. The diameters of the corresponding regions in real space, i.e., 2π divided by the Q-space diameter of the Gaussian part of the EISF, are shown in Fig. 4.

Uncertainties due to fitting error arising from counting statistics are comparable to, or smaller than, the size of the data points in Figs. 3 and 5–8 except for a few points, where larger standard deviation error bars are shown. Systematic errors, mainly arising from the presence of Bragg scattering from the sample, are typically larger, and are approximately 0.04 (standard deviation) in the elastic fractions of Figs. 3 and 6, and 0.3 μeV in the full widths at half maximum of Figs. 5, 7, and 8. The data of Figs. 3, 6, and 9 were corrected for scattering from the zeolite host by subtracting a constant amounting to 25–30 % of the apparent elastic fraction. There appears to be a change in the Q dependence of the FWHM data for 320 K in Fig. 5 relative to lower temperatures. We do not understand the reason for the change, but it may arise

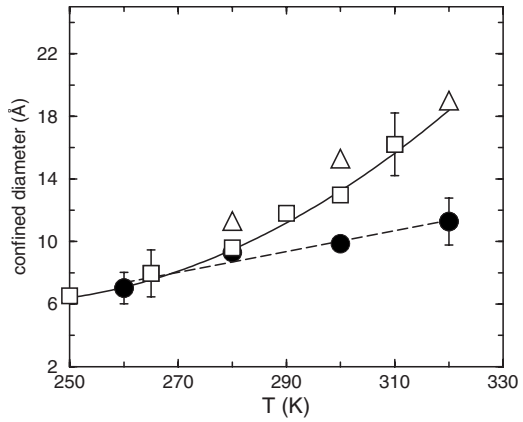

FIG. 4. Estimated confinement diameters (see text) for the mobile water fractions in NaX (open symbols) and NaA zeolite (filled symbols). For NaA, the hydration level corresponds to a fractional mass gain of 0.20. For NaX, the triangles are for a lower hydration level (0.22 fractional mass gain) than the squares (0.28 fractional mass gain). The error bars are intended to be standard deviations.

from the onset of longer-range diffusive jumps at the higher temperature.

The data of Fig. 3 indicate the coexistence of relatively mobile and immobile water molecules. The most obvious interpretation is that, at the highest temperatures, the immobile fraction is the water in the β cages, comprising approximately four molecules within each cage. This would lead us to expect a higher-temperature limit to the immobile fraction of around 0.2 for NaA and 0.1 for NaX, in reasonable accord with our data. Another reasonable interpretation is that the relatively immobile molecules are those in the immediate environment of the charged surfaces and sodium ions, i.e., the immobile molecules hydrate charge centers. In the latter case, we presume the effects of chemical bonding to be more important than purely geometrical constraints in restricting the motion of water molecules. The two pictures are not completely distinct, since molecules in the β cages are more likely to be close to charged surfaces and cations. As the temperature is lowered, more molecules become immobi-

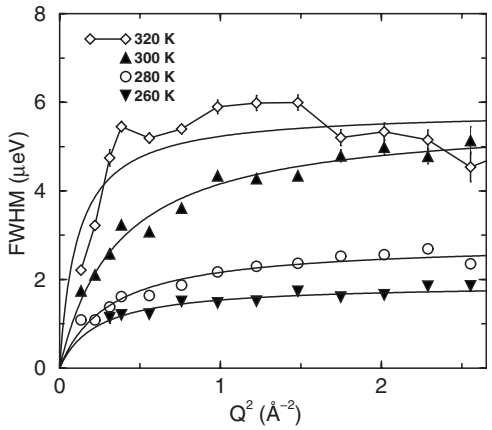

FIG. 5. Quasielastic widths for water in NaA zeolite. Fits are to Eq. (3), as described in the text. The hydration level corresponds to a fractional mass gain of 0.20 over the dry zeolite.

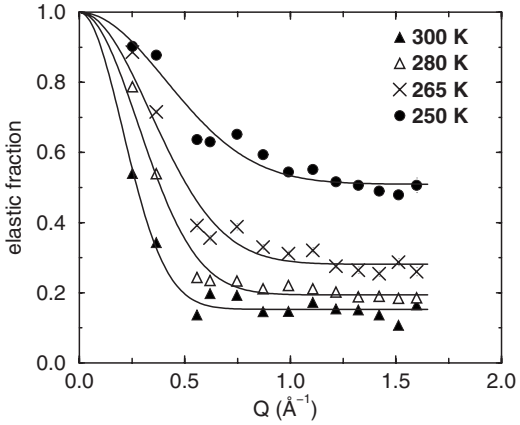

FIG. 6. Wave vector dependence of the apparent elastic fraction for scattering from water in NaX zeolite. Fits are to a constant plus a Gaussian centered at $Q=0$. Similar data and fitted curves were obtained at 310 and 290 K. The hydration level corresponds to a fractional mass gain of 0.22 over the dry zeolite.

lized, the last to do so being the ones closest to the centers of the α cages.

In either picture, at higher temperatures, most of the molecules in the α cages are relatively mobile within each cage, but diffuse more slowly to other cages. Thus we observe an apparent EISF reflecting the confinement. The apparently elastic component cannot be completely so, since water diffuses through the structure at temperatures around 300 K, permitting hydration and dehydration in humid air in minutes to hours. The confinement diameters shown in Fig. 4 for NaA are reasonable, given the uncertainties of fitting, i.e., they are comparable to the size of the α cages. The Gaussian shape for the distribution of confined water should not be taken literally. The distribution of mobile water is more likely to conform to the shape of the α cages, with lobes toward the channels to adjacent cages. However, the data are rather insensitive to the exact shape. For instance, the hard-walled spherical cavity model of Volino and Dianoux [37] predicts a shape for the EISF that is visually similar to a Gaussian, i.e.,

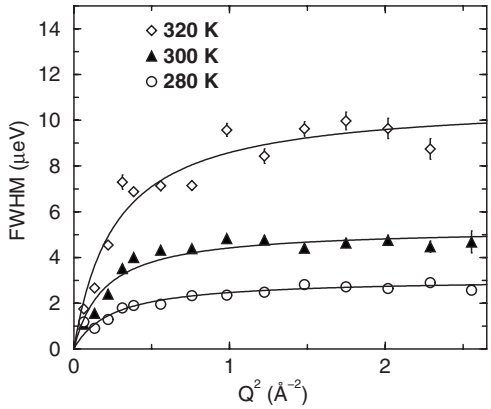

FIG. 7. Quasielastic widths for water in NaX zeolite. Similar data sets and fitted curves were obtained at 310, 290, and 265 K. The hydration level corresponds to a fractional mass gain of 0.20 over the dry zeolite.

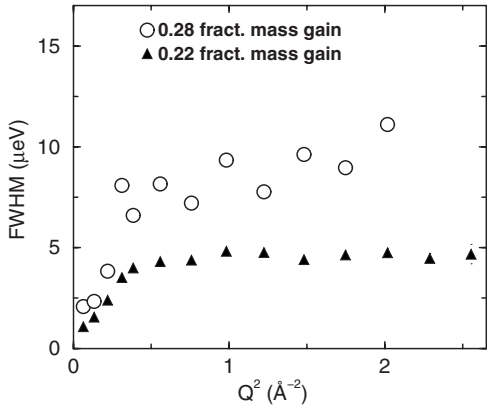

FIG. 8. Quasielastic widths at 300 K for water in NaX at two hydration levels.

$$A(q) = [3j_1(QR)/(QR)]^2, \tag{2}$$

where $j_1(x)$ is a spherical Bessel function, and R is the radius of the cavity. The confinement diameters $2R$ fitted to Eq. (2) would be about 11% larger than the Gaussian diameters of Fig. 4. Fitting the NaA data to a spherical shell form factor, i.e., $[\sin(QR)/(QR)]^2$, gives values for the diameters about 15% smaller than fitting the EISF to a Gaussian. In all three types of fits, the values are physically reasonable. The quasielastic widths observed for the mobile water component in NaA, shown in Fig. 5, are somewhat smaller than the widths observed for most other aqueous systems that have been investigated by QENS at comparable temperatures. For example, the full width at half maximum (FWHM) for bulk water at 300 K and $Q=0.8$ Å^{-1} is 180 μeV, about 50 times larger than the corresponding width for water in NaA. Between these extremes are widths observed for water confined within porous silica [2–10] and interlayer water in layered silicates [11–15]. The widths for NaA increase with Q at each temperature, but tend to saturate at high Q, indicating diffusive motions that are jumplike, with fairly long residence times between relatively fast jumps.

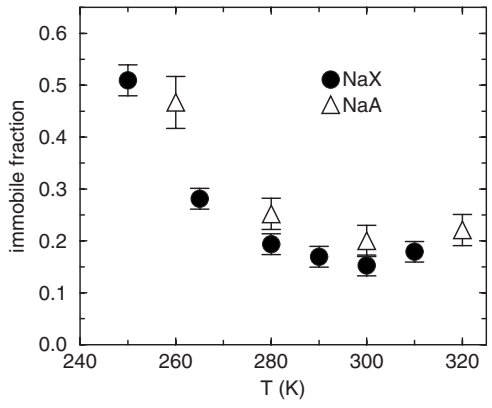

FIG. 9. Temperature dependence of immobile water fraction for water in NaA and NaX zeolites. The error bars are intended to be standard deviations. The hydration levels correspond to fractional mass gains of 0.20 for the NaA sample, and 0.22 for the NaX sample.

TABLE I. Local diffusion coefficients D, residence times τ_0, and jump lengths $L=(6D\tau_0)^{1/2}$ obtained by fitting the simple jump-diffusion model to the QENS spectra. Error estimates are intended to be two standard deviations. The hydration levels correspond to fractional mass gains of 0.20 for NaA, 0.22 for NaX-1, and 0.28 for NaX-2.

Sample	T (K)	$D(10^{-9}$ m^2 s$^{-1})$	(ns)	L (nm)
Hydrated	260	0.12 ± 0.08	0.35 ± 0.05	0.50 ± 0.15
NaA	280	0.14 ± 0.08	0.23 ± 0.04	0.44 ± 0.10
	300	0.24 ± 0.12	0.12 ± 0.02	0.41 ± 0.10
Hydrated	280	0.19 ± 0.08	0.21 ± 0.03	0.49 ± 0.10
NaX-1	300	0.40 ± 0.12	0.12 ± 0.02	0.55 ± 0.10
	320	0.62 ± 0.15	0.061 ± 0.015	0.48 ± 0.10
Hydrated	250		0.29 ± 0.04	
NaX-2	265		0.25 ± 0.03	
	280	0.24 ± 0.12	0.13 ± 0.02	0.44 ± 0.10
	290	0.46 ± 0.15	0.077 ± 0.01	0.46 ± 0.10
	300	0.45 ± 0.15	0.048 ± 0.01	0.36 ± 0.10
	310	0.59 ± 0.20	0.043 ± 0.01	0.39 ± 0.10

Fitting the widths to a simple jump diffusion model [39], i.e.,

$$2\Gamma = 2DQ^2/(1 + DQ^2\tau_0), \tag{3}$$

where τ_0 is an average residence time between jumps, D is the diffusion coefficient, and 2Γ is the full width at half maximum, works well for the three lower temperatures, but not for 320 K. The model is inadequate in several other respects, and we use Eq. (3) mainly as a convenient global fitting procedure, although the parameters we obtain from it appear to be physically reasonable. However, we recognize that it is an oversimplification to assume a single relaxation time, since the environment experienced by a water molecule in zeolites is complex, and also that Eq. (3) neglects the effects of confinement. Among the latter must be the appearance of an elastic incoherent structure factor, and of a finite value of the quasielastic width at very small Q. The Volino-Dianoux model [37], discussed previously, is inappropriate in other respects, in that it treats continuous random diffusion in a sphere, in contrast to the jumplike motion indicated by our data. However, it should be valid in the $Q=0$ limit, where it predicts a finite width of $4.33D/R^2$ due to confinement. Our data do not extend to sufficiently small Q to determine whether the widths approach a finite value.

Parameters obtained by fitting Eq. (3) to our data are shown in Table I. One should consider D to be a local diffusion coefficient, characteristic of intracage motion. The values of D are not accurately determined by the data, especially for NaA, and for lower temperatures for NaX, since the curves flatten out quickly with Q^2 and the low-Q limit has a large uncertainty. The fitted values of D are about five to ten times smaller than for bulk water at the same temperatures. The values of τ_0 are better determined than those of D, since the former is determined by the limiting value of the

FWHM at large Q, i.e., $2/\tau_0$. The values of the mean jump length $L=(6D/\tau_0)^{1/2}$ are not as well defined as those of τ_0, but consistently lie in the range of 4–5 Å, considerably larger than the distances found for bulk water (1–2 Å) [36], or for water confined in porous silica glass (0.5–1 Å) [6]. Arrhenius fits to the residence times give activation energies of 0.16 eV for hydrated NaA, 0.22 eV for the NaX sample at lower hydration, and 0.19 eV for the NaX sample at higher hydration. The values are the same within the 2σ estimated error of 0.04 eV, and comparable to values obtained for bulk or confined water.

Several molecular dynamics (MD) studies of water motion in zeolites provide useful insights for the interpretation of our data. Most directly relevant is a simulation of water in NaA by Faux [27] at several hydration levels. It predicts that diffusive motion becomes faster with increasing water content, as we observe. At very high water content, saturation and slowing is predicted, due to self-blocking of the water molecules. The diffusion coefficients predicted, e.g., 0.5×10^{-9} m^2 s^{-1} at 298 K and 0.18 water mass fraction, are somewhat larger than indicated in the fits to our data, which give $0.24\pm0.12\times10^{-9}$ m^2 s^{-1} under the same conditions. Pulsed-field-gradient NMR for water in fully hydrated NaA [40] gives a diffusion coefficient about a factor of 2 smaller than our fits of Table I and several times smaller than the MD simulation, but this might be expected, since the former probes motion over larger distances. Faux notes that his simulation of bulk water using similar methods also gives a higher diffusion coefficient than observed (4.4×10^{-9} m^2 s^{-1} simulated, 2.5×10^{-9} m^2 s^{-1} observed). As in an earlier study [28] by Faux *et al.*, the water molecules in the simulation show a preference for locations on the periphery of the α cage, concentrating near sites interior to four, six, and eight rings. Regions of high probability of occupation are separated by about 1.7 Å. The latter distance is smaller than the 4–5 Å jump distances in our fits, suggesting that jumps occur mainly to more distant sites rather than between adjacent regions. Faux *et al.* propose an arrangement of 44 preferred sites for water in the α cage, of which only 32 can be simultaneously occupied. Noting the lack of exact correspondence with the pattern indicated in the x-ray structural study by Gramlich and Meier [31], Faux *et al.* suggest that their MD-derived arrangement might match the x-ray data as well. They also observe that the water in the β cages, comprising about 15% of the molecules, is immobile in the time scale of the simulation, in accord with our own observation of immobile water. An earlier simulation [30] of hydrated NaA zeolite predicts local diffusivities much higher than in bulk water, in marked contrast to our experiment. A recent simulation of water in NaX and NaY by Shirono *et al.* [29] at a number of water loadings predicts diffusion coefficients that are larger for the less-highly charged NaY, and first rise, then decline with water content as self-blocking increases. Their values for the diffusion coefficient at comparable hydration levels at 300 K are smaller by a factor of 2 to 3 than given by our fits in Table I. A new molecular dynamics simulation of the conditions of the present experiments, including calculation of the scattering functions, would be informative, and might permit a more detailed interpretation of the QENS data.

The apparent EISFs observed for NaX (Fig. 6) are similar to those obtained for NaA, except that the rise at small Q occurs at a lower wave vector, indicating confinement to a larger volume. The temperature dependence of confinement diameters fitted to the data (Fig. 4) gives reasonable values, around the size of the α cage in NaX. The fraction of immobile water molecules is somewhat smaller in the NaX sample than in NaA. This is also reasonable, since the larger α cage of NaX can accommodate a greater number of mobile molecules. The widths observed for the fully hydrated NaX sample (Fig. 7) are about twice as large as observed for NaA at a given temperature. However, we observe that the magnitude of the broadening is sensitive to the hydration level, so the difference cannot be attributed solely to characteristics of the zeolite material. Figure 8 compares quasielastic widths for water in NaX at two hydration levels, i.e., 22% and 28% mass increase on hydration. The widths are about a factor of 2 larger at the higher hydration level.

The temperature dependence of the immobile fraction (Fig. 9) is very similar for NaA and NaX. In both cases, it remains roughly constant from 320 K down to 280 K, and increases below that temperature as the absorbed water gradually freezes. Although the diffusion in NaX is considerably faster than in NaA, this representation shows only a modest temperature displacement of the curves with respect to each other of around 7 K. If we take the temperature at which the immobile fraction reaches 0.5 as an average freezing "point," the depression of the latter with respect to bulk water is about 15 K for NaX and 22 K for NaA. One should note that such a characterization depends on the resolution of the instrument. Poorer resolution will result in an apparently smaller depression, since more molecules will appear immobile at higher temperatures.

Finally, we return to consideration of whether fits to alternative QENS line shapes might affect the interpretation of the data. For several data sets, we fit spectra to the Kohlrausch-Williams-Watt (KWW) function, a line shape that is the Fourier transform of stretched-exponential decay $\exp(-t/t)^{\beta}$, and a frequent choice for the analysis of QENS data. As applied to water and water in confinement [3] in the context of the theory of glasses and the "relaxing cage model" [4], the KWW provides excellent fits to the quasielastic spectra. The KWW has two disposable parameters, τ and β, instead of one for a Lorentzian, which is a special case of the KWW with $\beta=1$. In general, we found that τ and β did not converge to well-defined values if one allowed an elastic component as was done for our Lorentzian fits. If the value of β is fixed, then the elastic fraction and τ converge to well-defined values. Thus the value we assign to the elastic fraction for a specific spectrum can be considered a function of β. If no elastic component is allowed, somewhat poorer, but still reasonable, fits are obtained, but with very small β, typically around 0.2 or less. This is understandable, since a small value of β will produce a highly peaked line shape with broad wings, indistinguishable within resolution from the combination of a less-peaked function with a central sharp component. However, the physical interpretation no matter what value of β we accept is similar. That is, there is a central component arising from relatively immobile water molecules comprising about 10–30 % of the integrated inten-

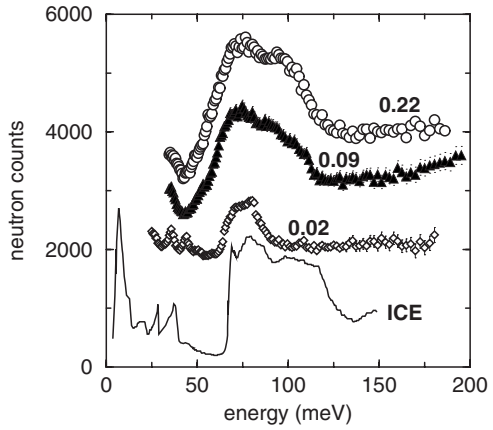

FIG. 10. Librational mode spectra for water at 12 K in NaA zeolite at three hydration levels. The lower, middle, upper, and middle spectra have been shifted upward by 1500, 2000, and 2500 counts, respectively. The data for ice (on an arbitrarily adjusted vertical scale) are from Ref. [43].

sity for most of our spectra. In the case of a KWW fit with small β, the sharp central component arises from the KWW function itself, originating from a broad distribution of relaxation times with some very long ones. Fitting a Lorentzian and an elastic component more simply apportions the intensity into two parts: one with a single relaxation time, and another with relaxation times too long to measure on the instrument. Using the latter procedure is, we believe, the most convenient, reliable, and consistent way of comparing our spectra for different wave vector, temperatures, and hydration levels.

IV. VIBRATIONAL SPECTROSCOPY

A different neutron scattering method [41] may be applied to investigate much faster motions of the water molecules. The filter analyzer neutron spectrometer (FANS) is used to measure energy transfers between 25 and 200 meV, conveniently spanning the range of librational modes in aqueous media, which occur from 40 to 160 meV. In this technique, the incident neutron energy is scanned, and all neutrons scattered to energies below the 1.2 meV cutoff energy of a low-pass filter material (polycrystalline graphite) are detected. Measurements were made on a NaA sample with varying degrees of hydration, 2, 9, and 22 % by weight. All data were taken at a sample temperature of 12 K. At a high hydration level, the librational mode spectrum (Fig. 10) is similar to that of ordinary ice, but shifted to lower energies by about 10 meV. For lower hydration, the shoulder at 100 meV becomes weaker, and finally, at a very low hydration level of about 2% by weight, the spectrum is sharper and centered at 80 meV. The two top spectra in Fig. 10 are similar to spectra for various forms of ice [42,43], but the features are less distinct. It is evident that the hydrogen bonding among water molecules in NaA influences the librational dynamics much as it does in ice, producing a wide band of excitations that correspond to dispersive phonons in crystalline ice, but the environment is more heterogeneous. The leading edge of the librational band is broader than for crystalline ices, and similar to spectra of amorphous forms, indicating greater disorder in the bonding. At very low hydration levels, i.e., for the spectrum second from the bottom in Fig. 10, the intermolecular H bonding becomes weak and molecules tend to be located in definite sites in the structure, almost certainly in the β cages, sharpening the librational spectrum, which arises from H bonding to the zeolite framework and/or to Na^+ cations. Corsaro *et al.* [44,45] have also recently measured vibrational spectra for water in NaA. Their results for the librational spectra are similar to ours, and in addition, they report spectra for Mg-exchanged A zeolites that show a hardening of the librational modes upon the substitution of Mg^{++} for Na^+. The residual water molecules have a strong affinity for the Na^+ cations, so that the spectrum that we observe at low hydration levels is likely that of molecules in close proximity to the cations. In addition to the librational modes, we see sharp low energy peaks at 36 and 45 meV. The latter are similar to features observed for water in small-pored zeolites by Line *et al.* [46], who assigned them to modes of water-cation complexes. A mode at lower energy, 4 meV, has been observed for water in NaA by Trouw *et al.* [47], who assigned it to a center-of-mass translational mode of the water-Na complex.

V. PERSPECTIVE AND SUMMARY

Numerous QENS investigations of molecular motion in zeolites, mostly involving organic molecules, have been reported. Studies on small molecules [48–50] show some behavior qualitatively similar to that of water in NaA and NaX, and some noteworthy differences. For instance, a gradual freezing over a wide temperature range is observed for H_2 in NaA, rather similar [48] to the behavior we have described for water in zeolites. For methane [49] in NaA, one observes an apparent EISF characteristic of the α-cage radius (minus the radius of the methane molecule), with some indications of a progressive freezing reflected in an increase in the elastic intensity at large Q. A more recent study of benzene [50] in NaX and NaY shows that diffusivities decrease as the loading is increased from 1.5 to 4.0 molecules per α cage, and is two orders of magnitude lower in NaY than in NaX. The former is a faujasitic structure zeolite, like NaX, but has a higher Si/Al ratio, on the order of 2.5 rather than 1.25. Both trends observed for benzene in NaX and NaY are opposite in sign to our observations for water in zeolites, where we see higher loading and a less highly charged environment promoting faster diffusive motions.

More closely related to the current study are QENS experiments on water in zeolites, clay minerals, and porous glasses, and a number of computer simulations. In experiments on hydrated zeolites analcime [19], Zeolite-P [18], harmotome [20], the resolution employed was between 35 and 50 μeV. With the exception of the study on harmotome, the quasielastic scattering in all these cases is substantially narrower than in bulk water, as we observe, and also as observed in many experiments on related materials such as clay minerals and porous silica glasses. The quasielastic scattering observed at relatively low resolution tends to be dominated by the rotational component, as noted in Refs. [18] and

[19]. In a recent study of water in NaX (zeolite M-3135) at 15 μeV resolution, Swenson *et al.* [21] observe a slowing of the dynamics relative to bulk water of about a factor of 30 at 295 K. Swenson *et al.* also made neutron spin echo, effectively very high resolution, measurements on D_2O in NaX.

With the higher resolution used in our experiment (1 μeV), rotational quasielastic broadening and translational motion of the most mobile molecules observed at lower resolution tends to look like background on our spectra, while the broadening we observe would appear elastic at lower resolution. Comparing our results with data on water in NaA reported by Crupi *et al.* [23] at much lower (54 μeV) resolution, we note that in the latter study, a relatively high fraction of the scattering (more than 0.8) appears elastic, and the quasielastic scattering shows features associated with water confined to a small volume, around 3 Å in diameter at 273 K. We infer that the authors of Ref. [23] are observing the relatively rapid motion of a few molecules per α cage at the centers of the cages, while we are mainly measuring the dynamics of a larger number of molecules around the peripheries of the cages. In a subsequent study [25] at somewhat higher resolution, i.e., 18 μeV, a smaller fraction appears elastic, and the confinement diameter appears to increase to 5 or 6 Å at 293 K. Our study is not sensitive to the large QENS broadening observed in Refs. [23] and [25], but we recognize that we are characterizing the translational diffusive motions of most, but not all, of the confined water molecules. Recent experiments on NaA and NaCaA [24] using high resolution (1 μeV) show widths consistent with what we observe, given that the water loadings in Ref. [24] are lower and temperatures higher than the conditions of our experiment. The Ca substitution and lower water content both result in slower motions, again consistent with our current data on the effects of charge and hydration level on the dynamics.

We note that Mamontov [51–53] has reported QENS experiments for water adsorbed on nanoparticles of CeO2 and ZrO2, observing diffusional behavior rather similar to our picture for water in zeolites. At high resolution (1 μeV), the slow dynamics of the innermost adsorbed layer is observed [51], approximately two orders of magnitude slower than bulk water, whereas at lower resolution (19 μeV), the QENS [52] is due to outer hydration layers, arising from motions an order of magnitude faster than in the inner layer.

In a direct comparison of QENS data on hydrated silica-based materials, bulk water, and aqueous solutions, we note that the presence of ions and charged silicate surfaces appears to have a dominant effect in determining the rapidity of the diffusive motion of water molecules. In Fig. 11, we have plotted the observed quasielastic line width at 300 K and a wave vector transfer $Q=0.8$ Å^{-1} for bulk water [3] and water in a number of siliceous host materials. The abscissa in the figure is the cation charge per water molecule, which is zero for bulk water and water in purely siliceous materials, and a number determined by the Si/Al ratio and hydration level for the aluminosilicate materials. The latter include two points for a synthetic layered silicate [6] (fluormica), with one and two water layers between silicate layers. In each case, the fitting was restricted to data from a single detector corresponding to $Q=0.8$ Å^{-1}. A reasonable interpretation of

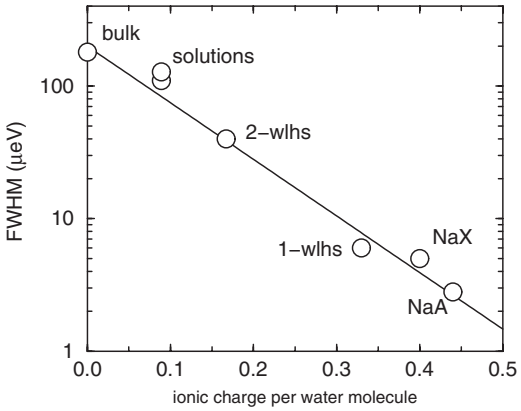

FIG. 11. The width of QENS line shapes at $Q=0.8$ Å^{-1}, $T=300$ K in (from right to left) hydrated NaA, hydrated NaX, fluormica in the one-water layer hydration state (1-wlhs), fluormica in the two-water layer state (2-wlhs), aqueous solutions of NaCl and NaI, and bulk water. The horizontal axis of the semilogarithmic plot is the charge per water molecule due to the host material or ions in solution.

Fig. 11 is that, if only a few water molecules are present, they are more strongly bound to charge sites, inhibiting diffusion. If more water molecules are present, those not immediately hydrating a charge site will diffuse more freely. In QENS studies of aqueous solutions [54], it has been shown that diffusive motions of water molecules are inhibited out to several hydration shells from various ions. Thus it is reasonable that the QENS width decreases as a function of charge concentration in Fig. 11. Two points for 5M aqueous solutions [55] of NaCl (upper point) and NaI (lower point) are also shown in the figure, immediately to the right of the point for bulk water. A restricted geometry can also have a slowing effect on the molecular motions. However, such effects are apparently smaller than the charge effect we have just discussed. The diffusion coefficient obtained from QENS for water in porous silica glass [2], i.e., Corning Vycor with tortuous, roughly cylindrical, pores of 50 Å average diameter, is comparable to bulk water at 298 K. In recent QENS studies [21] of MCM-41 and MCM-48 glasses with more uniform cylindrical pores, the effective diffusion coefficient of water adsorbed in 20–25 Å diameter pores is less than a factor of 2 smaller than in bulk water when measured at 1 μeV resolution on the HFBS. Lower resolution studies using neutron time-of-flight spectroscopy [54] indicate a more substantial slowing of factors of 4 or 5. By the measure of Fig. 11, the slowing in hydrated NaA or NaX relative to bulk water is nearly two orders of magnitude.

In summary, the small quasielastic widths observed in our experiment show that the local diffusive motion of water in zeolites is much slower than in bulk water, or in water confined within neutral microporous frameworks. In the NaA and NaX zeolites examined in this work, there is a relatively immobile water component, comprising 10–30 % of the molecules at temperatures between 280 and 320 K. The other molecules are relatively mobile within each α cage, but intercage diffusion is much slower, leading to the apparent EISF at small Q that we observe for water in both zeolites. As temperature is lowered below 280 K, more of the water

becomes immobile, and the apparent confinement diameter becomes smaller. At lower hydration levels in NaX, the diffusive motion is slower.

ACKNOWLEDGMENTS

The authors especially wish to thank Dr. Zema Chowdhuri and Dr. Robert Dimeo for help during the experiment on the NCNR backscattering spectrometer. We also wish to thank the Tohso Chemical Co. for providing the zeolite samples used in our measurements. N.W. is grateful to Toyo University for providing a special research fund for this work. Some commercial products are mentioned in this paper for the purpose of specificity in the description of our experimental procedures. This work utilized facilities supported in part by the National Science Foundation under Agreement No. DMR-0454672.

[1] M. Bée, *Quasielastic Neutron Scattering* (Adam Hilger, Bristol, Philadelphia, 1988).
[2] M. C. Bellissent-Funel, S. H. Chen, and J. M. Zanotti, Phys. Rev. E **51**, 4558 (1995).
[3] J. M. Zanotti, M. C. Bellissent-Funel, and S. H. Chen, Phys. Rev. E **59**, 3084 (1999).
[4] A. Faraone, L. Liu, C. Y. Mou, P. C. Shih, J. R. D. Copley, and S. H. Chen, J. Chem. Phys. **119**, 3963 (2003).
[5] A. Faraone, L. Liu, C. Y. Mou, C. W. Yen, and S. H. Chen, J. Chem. Phys. **121**, 10843 (2004).
[6] S. Takahara, M. Nakano, S. Kittaka, Y. Kuroda, T. Mori, H. Hamano, and T. Yamaguchi, J. Phys. Chem. B **103**, 5814 (1999).
[7] S. Takahara, N. Sumiyama, S. Kittaka, T. Yamaguchi, and M. C. Bellissent-Funel, J. Phys. Chem. B **109**, 11231 (2005).
[8] L. Liu, A. Faraone, C. Y. Mou, C. W. Yen, and S. H. Chen, J. Phys.: Condens. Matter **16**, S5403 (2004).
[9] L. Liu, S. H. Chen, A. Faraone, C. W. Yen, C. Y. Mou, A. I. Kolesnikov, E. Mamontov, and J. Leao, J. Phys.: Condens. Matter **18**, S2261 (2006).
[10] F. Mansour, R. M. Dimeo, and H. Peemoeller, Phys. Rev. E **66**, 041307 (2002).
[11] D. J. Cebula, R. K. Thomas, and J. W. White, Clays Clay Miner. **29**, 241 (1981).
[12] J. J. Tuck, P. L. Hall, M. H. B. Hayes, D. K. Ross, and C. Poinsignon, J. Chem. Soc., Faraday Trans. 1 **80**, 309 (1984).
[13] J. J. Tuck, P. L. Hall, M. H. B. Hayes, D. K. Ross, and J. B. Hayter, J. Chem. Soc., Faraday Trans. 1 **81**, 833 (1985).
[14] J. Conard, J. Estrade-Szwarckopf, A. J. Dianoux, and C. Poinsignon, J. Phys. (Paris) **45**, 1361 (1984).
[15] W. A. Kamitakahara and N. Wada, Mol. Cryst. Liq. Cryst. **341**, 503 (2000).
[16] J. Swenson, R. Bergman, and S. Longeville, J. Chem. Phys. **115**, 11299 (2001).
[17] S. Nair, Z. Chowdhuri, I. Peral, D. A. Neumann, L. C. Dickinson, G. Tompsett, H.-K. Jeong, and M. Tsapatsis, Phys. Rev. B **71**, 104301 (2005).
[18] P. D. Shepherd, W. W. Kagunya, S. I. Campbell, A. P. Chapple, J. W. Dreyer, R. J. Humphreys, M. Kemali, M. Mercer, and D. K. Ross, Physica B **234-236**, 914 (1997).
[19] C. M. B. Line, B. Winkler, and M. T. Dove, Phys. Chem. Miner. **21**, 451 (1994).
[20] R. Stockmeyer, Ber. Bunsenges. Phys. Chem **102**, 623 (1998).
[21] J. Swenson, H. Jansson, W. S. Howells, and S. Longeville, J. Chem. Phys. **122**, 084505 (2005).
[22] V. Crupi, D. Majolino, and V. Venuti, J. Phys.: Condens. Matter **16**, S5297 (2004).
[23] V. Crupi, D. Majolino, P. Magliardo, V. Venuti, U. Wanderlingh, T. Mizota, and M. Telling, J. Phys. Chem. B **108**, 4314 (2004).
[24] H. Paoli, A. Methivier, H. Jobic, C. Krause, H. Pfeifer, F. Stallmach, and J. Kärger, Microporous Mesoporous Mater. **55**, 147 (2002).
[25] C. Corsaro, V. Crupi, F. Longo, D. Majolino, V. Venuti, and U. Wanderlingh, Phys. Rev. E **72**, 061504 (2005).
[26] C. Corsaro, V. Crupi, D. Majolino, P. Migliardo, V. Venuti, U. Wanderlingh, T. Mizota, and M. Telling, Mol. Phys. **104**, 587 (2006).
[27] D. A. Faux, J. Phys. Chem. B **103**, 7803 (1999).
[28] D. A. Faux, W. Smith, and T. R. Forester, J. Phys. Chem. B **101**, 1762 (1997).
[29] K. Shirono, A. Endo, and H. Daiguji, J. Phys. Chem. B **109**, 3446 (2005).
[30] S. H. Lee, G. K. Moon, S. G. Choi, and H. S. Kim, J. Phys. Chem. **98**, 1561 (1994).
[31] V. Gramlich and W. M. Meier, Z. Kristallogr. **133**, 134 (1971).
[32] T. Ikeda, F. Izumi, T. Kodaira, and T. Kamiyama, Chem. Mater. **10**, 3996 (1998).
[33] D. H. Olson, Zeolites **15**, 439 (1995).
[34] D. H. Olson, J. Phys. Chem. **74**, 2758 (1970).
[35] C. E. A. Kirschhock, B. Hunger, J. Martens, and P. A. Jacobs, J. Phys. Chem. B **104**, 439 (2000).
[36] J. Teixeira, M. C. Bellissent-Funel, S. H. Chen, and A. J. Dianoux, Phys. Rev. A **31**, 1913 (1985).
[37] F. Volino and A. J. Dianoux, Mol. Phys. **41**, 271 (1980).
[38] A. Meyer, R. M. Dimeo, P. M. Gehring, and D. A. Neumann, Rev. Sci. Instrum. **74**, 2759 (2003).
[39] K. S. Singwi and A. Sjolander, Phys. Rev. **119**, 863 (1960).
[40] J. Kärger, H. Pfeifer, M. Rosenmann, N. N. Feokistova, and S. P. Zdanov, Zeolites **9**, 247 (1989).
[41] J. R. D. Copley, D. A. Neumann, and W. A. Kamitakahara, Can. J. Phys. **73**, 763 (1995).
[42] D. D. Klug, C. A. Tulk, E. C. Svensson, and C. K. Loong, Phys. Rev. Lett. **83**, 2584 (1999).
[43] A. I. Kolesnikov, J. C. Li, S. Dong, I. F. Bailey, R. S. Eccleston, W. Hahn, and S. F. Parker, Phys. Rev. Lett. **79**, 1869 (1997).
[44] C. Corsaro, V. Crupi, D. Majolino, S. F. Parker, V. Venuti, and U. Wanderlingh, J. Phys. Chem. A **110**, 1190 (2006).
[45] C. Corsaro, V. Crupi, F. Longo, D. Majolino, V. Venuti, and U. Wanderlingh, J. Phys.: Condens. Matter **17**, 7925 (2005).
[46] C. M. B. Line and G. J. Kearley, J. Chem. Phys. **112**, 9058 (2000).
[47] F. R. Trouw and D. L. Price, Annu. Rev. Phys. Chem. **50**, 571

(1999).
[48] R. Kahn, E. C. de Lara, and E. Viennet, J. Chem. Phys. **91**, 5097 (1989).
[49] E. C. de Lara and R. Kahn, J. Phys. (Paris) **42**, 1029 (1981).
[50] H. Jobic, A. N. Fitch, and J. Combet, J. Phys. Chem. B **104**, 8491 (2000).
[51] E. Mamontov, J. Chem. Phys. **123**, 024706 (2005).
[52] E. Mamontov, J. Chem. Phys. **121**, 9087 (2004).
[53] E. Mamontov, J. Chem. Phys. **123**, 171101 (2005).
[54] N. A. Hewish, J. E. Enderby, and W. S. Howells, J. Phys. C **16**, 1777 (1983).
[55] A. Tsai (unpublished).